Available online at http://scik.org
Commun. Math. Biol. Neurosci. 2023, 2023:62
https://doi.org/10.28919/cmbn/7924
ISSN: 2052-2541

A NEW COMPUTATIONAL MODELLING FOR PREDICTION OF COVID-19 POPULATION AND TO APPROXIMATE EPIDEMIC EVOLUTION OF THE DISEASE

C. F. CHOUKHAN[1,*], M. R. LEMNAOUAR[2], ELHATIMI[1], R. ZINE[3], O. IBRIHICH[1], M. ESGHIR[1]

[1]Laboratory of Mathematics Computing and Applications, Mohammed V University in Rabat, Faculty of Sciences, Rabat, Morocco

[2]LASTIMI, Mohammed V University in Rabat, Superior School of Technology, Salé, Morocco

[3]Laboratory of Mathematics Computing and Applications, School of Science and Engineering, Al Akhawayn University in Ifrane, Ifrane, Morocco

Abstract. Infectious diseases are growing at a fast rate. The early prediction and monitoring of the progress of such diseases, such as the recent outbreak of COVID-19, are fundamental to and infection control and rapid recovery. This paper presents (i) a new computational program based on a make blobs generator designed to predict the number of daily COVID-19 cases over a period of 30 days and (ii) a deterministic compartmental SEIQHRV model based on a system of ordinary differential equations. The objective of both the computational and mathematical models is to describe the dynamics of COVID-19 over time to understand the influence of specific parameters on its spread, while also predicting the approximate epidemic evolution of the disease. Furthermore, we evaluate and validate the new computational model by comparing our simulation results with the mathematical model, treating the latter as a reference model. Numerical simulations of the proposed models are applied to a randomly selected group of individuals. The results show that the curves obtained by the SEIQHRV mathematical model and those obtained by each scenario of the proposed computational model are approximately similar.

Keywords: COVID-19; mathematical model; computational modelling; make blobs.

2020 AMS Subject Classification: 26A33, 34A08, 34K37, 93C10, 93B52.

*Corresponding author

E-mail address: cherifafatima_choukhan@um5.ac.ma

Received February 22, 2023

1. INTRODUCTION

The outbreak of coronavirus disease 2019 (COVID-19) has led to one of the greatest global challenges in contemporary history, with more than 642 million infections and more than 6 million deaths worldwide [1]. While such health statistics are staggering, it would, however, be a serious mistake to describe this challenge only as a health crisis. It is a large-scale humanitarian crisis that has caused untold misery and human suffering, driving the socio-economic well-being of people to the brink of collapse. The COVID-19 pandemic has also had a significant negative influence on the global health system, leading many governments to adopt stringent measures to prevent the further spread of the epidemic and to ensure the proper functioning of their health systems [2]. Although the enforcement of such regulations and vaccines mitigated the effects of the pandemic initially, several vaccinated countries have recently seen a recurrence of the disease with new variations. Thus, the virus's extremely contagiousness and the emergence of harmful mutations are still impacting public health.

Understanding the nature of transmission and correctly forecasting the course of the epidemic are therefore two of the most crucial components in combating COVID-19, especially in countries with large populations. Furthermore, precise forecasting can provide feedback on whether an implemented policy is successful in reducing the strain on a particular nation's healthcare system. Governments can also use forecasts to evaluate mitigation strategies and regulate policies. For instance, by using mathematical models like the SIR and SEIR models, researchers have been able to accurately anticipate the COVID-19 reproduction parameter for the early prevention of the pandemic, thus highlighting the necessity for trustworthy forecasting models [3].

In this sense, mathematical models can be used to track the evolution of the epidemic by studying the behaviour of the virus. Using this approach, numerous researchers have examined COVID-19 from various perspectives [4, 5, 6, 7, 8]. Particulary, the study in [9] produced the traditional SEIR model, also known as fractional models for the examination of the global epidemic of COVID-19. The establishment of new quarantine regulations and the hospitalisation of infected patients (SEIQR model), which are regarded as epidemic parameters for COVID-19, are the foundations of this development [10]. Xu et al. [11] used the generalised fractional order

SEIR model to forecast the epidemic trend of COVID-19 in the USA. Two improved models, SEIQRP and SEIQRPD, then successfully captured the development process of COVID-19, providing an important reference for comprehending the trend of the outbreak. Meanwhile, the authors of [12] propose an optimal control problem based on a SEUIRD model adapted to the COVID-19 pandemic, which takes into consideration the epidemiological situation in Morocco. Furthermore, Ould Beinane et al. [13] studied the dynamics of the COVID-19 model SEIQHR with a standard incidence rate, considering fractional Caputo derivatives in order to gain a better insight into the disease.

Based on the aforementioned findings and previous literature, with the lack of effective treatment for COVID-19, vaccination is still one of the possible solutions for managing this infectious disease. In order to assess the impact of a vaccine programme on COVID-19 transmission, we propose an an extension of the classical models by using them to review the impact that vaccination has on infection rate hospitalised individuals (H), quarantined individuals (Q), and recovered individuals (R). The SEIQHRV goal of the epidemic model is to describe the dynamic behaviour of the disease and predict its propensity to spread.

The literature on this topic has until now indicated that mathematical modelling can play a crucial role in forecasting, detecting, and preventing COVID-19, while certain artificial intelligence approaches [14, 15, 16] can be used to estimate future COVID-19 viral transmission. See, for example, machine learning models (a hybrid approach based on a regression tree [17], long short-term memory (LSTM) networks [18], polynomial neural network (PNN) [19], FPASSA-ANFIS [20], SVR [21], etc.), and other types of models [22]. Another study [23] used deep learning to anticipate the pandemic trend for Brazil, India, and Russia – three nations that rank among the top ten in terms of global impact according to a thorough analysis by healthcare professionals. To forecast the number of cases and the spread of COVID-19 in these countries, three distinct deep learning models were used. In [24], the authors proposed a multi-source deep transfer learning-based novel approach to robustly forecast the COVID-19 transmission in a province within a country.

Additionally, significant progress has been made in detecting, preventing, and predicting COVID-19's harmful effects via computational, dynamic, and AI models, as well as in the use

of numerous technologies. Although epidemiological models help to assess the dynamics of progression, they make various assumptions and rely on the knowledge of various specific factors. To the best of our knowledge, no attempts to overcome these restrictions have yet been made, with no work being published that uses the characteristics of mathematical models to create a computational model (programmed in Python) to predict the growth of the COVID-19 population and to approximate epidemic evolution. Therefore, it is necessary to construct prediction techniques for frequent diseases, as well as to further expand prediction methodologies. The objective of the present study is to address this need.

The intended contributions of this work are as follows:

- We aim to create a new computational model similar to the traditional mathematical model based on a make blobs generator, which generates a feature matrix and corresponding discrete targets, and is used to demonstrate clustering.
- The proposed computational and mathematical models have the same objective: to study the transmission dynamics of COVID-19 and to simulate its propagation within a population of individuals. We will investigate several rates that make up our model to better understand how they affect the virus's pace of spread. This modelling will be implemented with the Plotly library [25].
- The computational model will then be compared to the SEIQHRV mathematical model, which belongs to the family of compartmental models in epidemiology.

The applicability of the proposed model will be assessed by simulating a population of 100,000 individuals. The information they provide and the situations in which the models are used show that the predictions produced by the two models are similar.

An overview of the paper's structure is provided below:

The first two sections cover the description of the two models. We begin by analysing the qualitative properties of the SEIQHRV mathematical model, including the bornitude of solutions and the disease-free and endemic equilibrium points. We then establish the conditions for the local asymptotic stability of the disease-free and endemic equilibrium points, before explaining the computational model. After that, we discuss the experimental findings in the results and discussion section, demonstrating how both approaches (mathematical and computational) affected

the behaviour of the different compartments. Finally, we describe a sensitivity analysis of the infection parameters, which we conducted in order to determine the impact of each parameter.

2. METHODS

Using previous knowledge of the COVID-19 pandemic, we propose a SEIQHRV model and a computational model to estimate the virus's epidemic spread. The computational model we propose differs from the traditional SEIQHRV model but produces relatively similar results to the mathematical model. In this section, we will provide a brief description of the two proposed models.

2.1. SEIQHRV model.

We employ a mathematical formulation built on differential equations to examine the transmission dynamics of COVID-19. The model separates the entire population into seven classes: susceptible individuals (S), exposed individuals (E), infected individuals who were not hospitalised (I), hospitalised individuals (H), quarantined individuals (Q), and recovered individuals (R). In addition, the model includes a compartment for vaccinated individuals (V). Individuals in the exposed class (E) are considered to be incubating; that is, even if they have no symptoms and have not tested positive for the disease, they are still contagious. The typical recommendation is for class (I) infected patients who tested positive but only have mild to moderate symptoms to self-quarantine at home rather than being admitted to hospital. People in class (H) who tested positive and are in hospital are more vulnerable (e.g. the elderly and those with underlying health problems). The parameters are described in Table 1 and the interactions between the compartments are illustrated in Figure 1. Our proposed model (2.1) can be presented in the following form:

$$
\left\{
\begin{array}{rcl}
\dfrac{dS}{dt} &=& \Lambda - \beta_1 SI - \beta_2 SE - a_s S - dS, \\
\dfrac{dE}{dt} &=& \beta_1 SI + \beta_2 SE - \alpha E - dE, \\
\dfrac{dI}{dt} &=& \alpha E - \delta I - \eta I - \mu I - dI, \\
\dfrac{dQ}{dt} &=& \delta I - \varepsilon Q - dQ, \\
\dfrac{dH}{dt} &=& \varepsilon Q + \eta I - rH - dH, \\
\dfrac{dR}{dt} &=& rH + \mu I - a_r R - dR, \\
\dfrac{dV}{dt} &=& a_s S + a_r R - dV.
\end{array}
\right. \tag{2.1}
$$

with initial conditions:

$$
S(0) \geq 0, E(0) \geq 0, I(0) \geq 0, Q(0) \geq 0, H(0) \geq 0, R(0) \geq 0 \text{ and } V(0) \geq 0. \tag{2.2}
$$

The following schema illustrates a detailed description of our model (2.1):

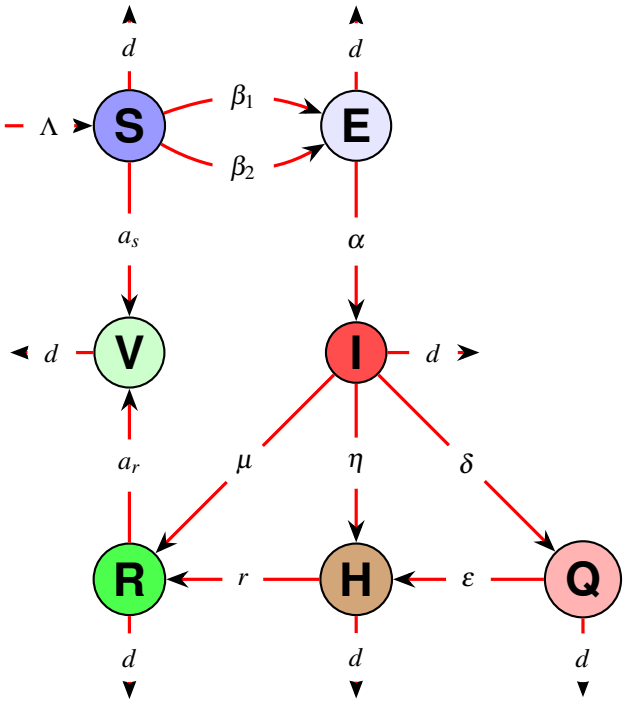

FIGURE 1. Schematic diagram of model (2.1)

The signification of these parameters and variables is shown in Table 1:

Parameters and variables	signification
S	Susceptible individuals
E	Exposed individuals
I	Infected individuals
Q	Quarantined individuals
H	Hospitalised individuals
R	Recovered individuals
V	Vaccinated individuals
Λ	Inflow number of susceptible individuals
β_1, β_2	Infection rates of the infected individuals and the exposed individuals, respectively
α	Incubation rate
δ	Rate at which symptomatic infections are diagnosed and quarantined
d	death rate caused by the disease
d_s	death rate caused by the vaccine
μ	Rate at which symptomatic infections are diagnosed and recovered
η	Rate at which symptomatic infections are diagnosed and hospitalised
ε	Transition rate of quarantined individuals to the hospitalised infected class
r	Transition rate of hospitalised individuals to the recovered class
a_s	Transition rate of susceptible individuals to the vaccinated class
a_r	Transition rate of recovered individuals to the vaccinated class
$\beta_1 SI$, $\beta_2 SE$	Describe the transmission of diseases

TABLE 1. Explanations of the parameters and variables

2.2. Boundedness and positivity of solutions.

In this section, we will proof the boundedness of the solutions of our model (2.1).

Lemma 2.1. *The solutions of the system (2.1), which belongs in $\mathbb{R}^7_+$, are non-negative and uniformly bounded.*

Proof. We pose $\mathcal{N}(t) = S(t) + E(t) + I(t) + Q(t) + H(t) + R(t) + V(t)$, then

$$\frac{d\mathcal{N}}{dt} + d\mathcal{N} = \Lambda,$$

Using the theory of differential equation [26, 27], we obtain

$$\mathscr{N}(t) = \mathscr{N}(0)e^{-dt} + \frac{\Lambda}{d}\left(1 - e^{-dt}\right),$$

if $t \to \infty$, we have $0 < \mathscr{N}(t) \leq \mathscr{N}(0) + \frac{\Lambda}{d}$, demonstrating this Lemma. □

2.3. Disease-free equilibrium.

2.3.1. *Disease-free equilibrium.*

In order to find the equilibrium points, the equations of our system (2.1) must equal zero. It is clear that system (2.1) always has an infection-free equilibrium, as denoted by $P_0 = (S^0, E^0, I^0, Q^0, H^0, R^0, V^0)$, and which is given by $P_0(\frac{\Lambda}{d+a_s}, 0, 0, 0, 0, 0, \frac{a_s\Lambda}{d(d+a_s)})$.

2.3.2. *Basic reproduction number.*

The reproduction number R_0 for the dynamics of disease is calculated using the next-generation method. Let $x = (E, I, Q, H)^t$, then we have $\frac{dx}{dt} = F - V$, where

$$F = \begin{pmatrix} \beta_2 S^0 & \beta_1 S^0 & 0 & 0 \\ 0 & 0 & 0 & 0 \\ 0 & 0 & 0 & 0 \\ 0 & 0 & 0 & 0 \end{pmatrix} \text{ and } V = \begin{pmatrix} \alpha + d & 0 & 0 & 0 \\ -\alpha & \delta + \eta + \mu + d & 0 & 0 \\ 0 & -\delta & k + d + \varepsilon & 0 \\ 0 & -\eta & -\varepsilon & r + d \end{pmatrix}.$$

After calculation, the spectral radius of the next generation matrix $p(FV^{-1})$ is shown by

$$R_0 = \frac{\Lambda(\beta_1\alpha + \beta_2(\delta + \mu + \eta + d))}{(d + a_s)(\delta + \mu + \eta + d)(\alpha + d)}. \tag{2.3}$$

2.4. Endemic equilibrium and local Stability.

First, we find the coordinates of the endemic equilibrium point, after which we will analyse the local stability of the two equilibrium points.

Theorem 2.1. *If $R_0 > 1$, then model (2.1) has endemic equilibrium point $P^*(S^*, E^*, I^*, Q^*, H^*, R^*, V^*)$, where $(S^*, E^*, I^*, Q^*, H^*, R^*, V^*)$ are defined after in (2.4).*

Proof. For the equilibrium points of model (2.1), we have

$$\frac{dS}{dt} = \frac{dE}{dt} = \frac{dI}{dt} = \frac{dQ}{dt} = \frac{dH}{dt} = \frac{dR}{dt} = \frac{dV}{dt} = 0.$$

Then we get:

$$
\begin{aligned}
S^* &= \frac{\Lambda(\delta+\mu+d+\eta)}{\beta_1\alpha E^*+(\beta_2 E^*+d+a_s)(\delta+\mu+d+\eta)},\\
I^* &= \frac{\alpha E^*}{\delta+\mu+d+\eta},\\
Q^* &= \frac{\delta\alpha E^*}{(k+d+\varepsilon)(\delta+\mu+d+\eta)},\\
H^* &= \frac{[\eta(\varepsilon+k+d)+\varepsilon\delta]\alpha E^*}{(k+d+\varepsilon)(r+d)(\delta+\mu+d+\eta)},\\
R^* &= \frac{(r[\eta(\varepsilon+k+d)+\varepsilon\delta]+\mu(r+d)(k+d+\varepsilon))\alpha E^*}{(k+d+\varepsilon)(r+d)(\delta+\mu+d+\eta)(d+a_r)},\\
E^* &= \frac{(\delta+\mu+d+\eta)(d+a_s)}{\beta_1\alpha+\beta_2(\delta+\mu+d+\eta)}(R_0-1),\\
V^* &= \frac{a_s S^*+a_r R^*}{d}.
\end{aligned}
\tag{2.4}
$$

Then, if $R_0 > 1$, then model (2.1) has endemic equilibrium point $P^*(S^*,E^*,I^*,Q^*,H^*,R^*)$, where $(S^*,E^*,I^*,Q^*,H^*,R^*)$ are defined before in (2.4). □

Now we analyse the local stability of two equilibrium points P_0 and P^*.
The Jacobian matrix associated with the model (2.1) is defined by

(2.5)
$$
J=\begin{pmatrix}
-(\beta_1 I+\beta_2 E+d+a_s) & -\beta_2 S & -\beta_1 S & 0 & 0 & 0 & 0\\
\beta_1 I+\beta_2 E & \beta_2 S-\alpha-d & \beta_1 S & 0 & 0 & 0 & 0\\
0 & \alpha & -(\delta+\eta+\mu+d) & 0 & 0 & 0 & 0\\
0 & 0 & \delta & -(k+d+\varepsilon) & 0 & 0 & 0\\
0 & 0 & \eta & \varepsilon & -(r+d) & 0 & 0\\
0 & 0 & \mu & 0 & r & -(d+a_r) & 0\\
a_s & 0 & 0 & 0 & 0 & a_r & -d
\end{pmatrix},
$$

Theorem 2.2. *The equilibrium point P_0 is locally asymptotically stable if $\delta+\mu+\eta+2d+\alpha > \frac{\beta_2\Lambda}{d}$ and $R_0 < 1$.*

Proof. We calculate the eigenvalues of the Jacobian matrix at the equilibrium point P_0 in order to analyse its local stability. Then, the characteristic equation of $P_0(\frac{\Lambda}{d},0,0,0,0,0,\frac{a_s\Lambda}{d(d+a_s)})$ is:

$$(\lambda+d)(\lambda+d+a_s)(\lambda+d+a_r)(\lambda+r+d)(\lambda+k+d+\varepsilon)(\lambda^2+s\lambda+p)=0,$$

where

$$
\begin{aligned}
s &= \delta+\mu+\eta+2d+\alpha-\tfrac{\beta_2\Lambda}{d+a_s},\\
p &= (\delta+\mu+\eta+d)(d+\alpha-\tfrac{\beta_2\Lambda}{d+a_s})-\tfrac{\alpha\beta_1\Lambda}{d+a_s},\\
&= (d+\alpha)(\delta+\mu+\eta+d)(1-R_0).
\end{aligned}
$$

The discriminant of equation $\lambda^2 + s\lambda + p = 0$ is $\left(\delta+\mu+\eta-\alpha+\frac{\beta_2\Lambda}{d}\right)^2 + \frac{4\Lambda\alpha\beta_1}{d} > 0$. Then, the eigenvalues of matrix (2.5) to the equilibrium point P_0 are reel roots, so :

$\lambda_1 = -(k+d+\varepsilon) < 0$, $\lambda_2 = -(r+d) < 0$, $\lambda_3 = \lambda_4 = -d < 0$, $\lambda_5 + \lambda_6 = -s$ and $\lambda_5\lambda_6 = p$.

If $s > 0$ and $R_0 < 1$, then $\lambda_5 + \lambda_6 < 0$ and $\lambda_5\lambda_6 > 0$. So $\lambda_5 < 0$ and $\lambda_6 < 0$. The proof is completed. □

Theorem 2.3. *The endemic equilibrium point P^* is locally asymptotically stable if $R_0 > 1$ $a_1, a_2 > 0$ and $a_1a_2 > a_0$ is realised.*

Proof. The eigenvalues of the Jacobian matrix associated with the equilibrium point P^* are calculated in order to study its local stability.

From the Jacobian matrix J^* (2.5), the characteristic equation at P^* is as follows:

$$(\lambda+d)(\lambda+d+a_r)(\lambda+r+d)(\lambda+k+d+\varepsilon)(\lambda^3+a_2\lambda^2+a_1\lambda+a_0) = 0,$$

where

$$\begin{aligned}
a_0 &= (\delta+\mu+\eta+d)\left((\beta_1 I^*+\beta_2 E^*+d)(\alpha+d)-d\beta_2 S^*\right)-\alpha d\beta_1 S^*,\\
a_1 &= (\delta+\mu+\eta+d)(\alpha+2d+\beta_1 I^*+\beta_2 E^*-\beta_2 S^*)+(\beta_1 I^*+\beta_2 E^*+d)(\alpha+d)\\
&\quad -(\beta_1\alpha+d\beta_2)S^*,\\
a_2 &= \beta_1 I^*+\beta_2 E^*+3d+\alpha-\beta_2 S^*+\delta+\mu+\eta.
\end{aligned}$$

Using (2.4), we get:

$$\begin{aligned}
a_0 &= dS^*(\alpha\beta_1+\beta_2(\eta+\mu+d+\delta))(R_0-1) > 0, \text{ because } R_0 > 1.\\
a_1 &= (\delta+\mu+\eta+\alpha+2d)dR_0-\tfrac{\beta_2\Lambda}{R_0},\\
a_2 &= \delta+\mu+\eta+\alpha+2d+dR_0-\tfrac{\beta_2\Lambda}{dR_0}.
\end{aligned}$$

$\lambda_1 = -(k+d+\varepsilon) < 0$, $\lambda_2 = -(r+d) < 0$, $\lambda_3 = -d < 0$.

Then, P^* is locally asymptotically stable if $R_0 > 1$, $a_1, a_2 > 0$, and $a_1a_2 > a_0$ are realised. □

2.5. Description of computational model.

In this section, we present a computational model (created in Python), designed specifically to predict the evolution of COVID-19-infected individuals over time based on a sample of random individuals. During the simulation, several parameters are taken into account. A population

of 100.000 individuals is chosen to provide a reasonable execution time. We assume that the entire population is likely to be contaminated. The distribution of these individuals is given by the parameter population variance, which varies between 0 and 2 approximately. The larger this parameter is, the wider the distribution of the population.

Then, the parameter radius contamination corresponds to the area in which an infected individual can spread the virus to an uninfected individual, with a probability named infectiousness (β_1; rate of individuals who become exposed without confirmation of infection and β_2; rate of individuals who become exposed with confirmation of infection). After being infected, there are three possibilities: an infected person can be hospitalised with a probability η, confined with a probability δ, or recover immediately with a probability μ. An individual can also be hospitalised in case of severity with a rate of ε and the passage of a hospitalised person recovered with a rate of r. These categories reflect the range of possible states of the population in the majority of real cases. We have considered the occurrence of vaccinations during the simulation, which relates to susceptible and recovered individuals with rates of a_s and a_r, respectively. A mortality rate d is imposed on all the categories of the individuals in our model.

The computational model is based on the make blobs generator, which produces a feature matrix, and the corresponding discrete targets. This generator creates multi-class datasets by assigning to each class one or more groups of normally distributed points. Make blobs allows better control of the centres and standard deviations of each group and is used to demonstrate clustering [28]. The simulations in this section are compiled using the Plotly library [25]. See the steps description diagram 2, which describes the core logic of the proposed model.

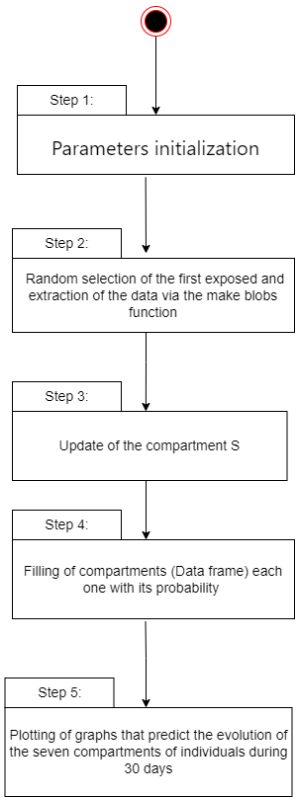

FIGURE 2. Steps of computational model.

Algorithm 2.1. *(1) Step 1*

Parameters initialisation

(2) Step 2

(a) Generated isotropic Gaussian blobs for clustering, created using make blobs.

(b) list_S: A two-dimensional data structure, i.e. data is aligned in a tabular fashion in rows and columns. list_S represents the coordination of each individual.

(c) A dictionary that holds the data of the curve and the coordination of each individual in certain compartments.

(d) Random selection of the first exposed individual from the susceptible individual group.

(e) Define distance between two points of the Cartesian plane.

(f) Thus chosing a random coordinate (individual) from the list 'list_S' to be the first infected person.

(g) Lists filling.

(h) Update of the compartment S.

(3) Step 3

(a) Clustering of compartments of individuals (data frame), each with its own probability. To provide a deeper insight, we present the clustering process of the first two compartments (see Figure 3)

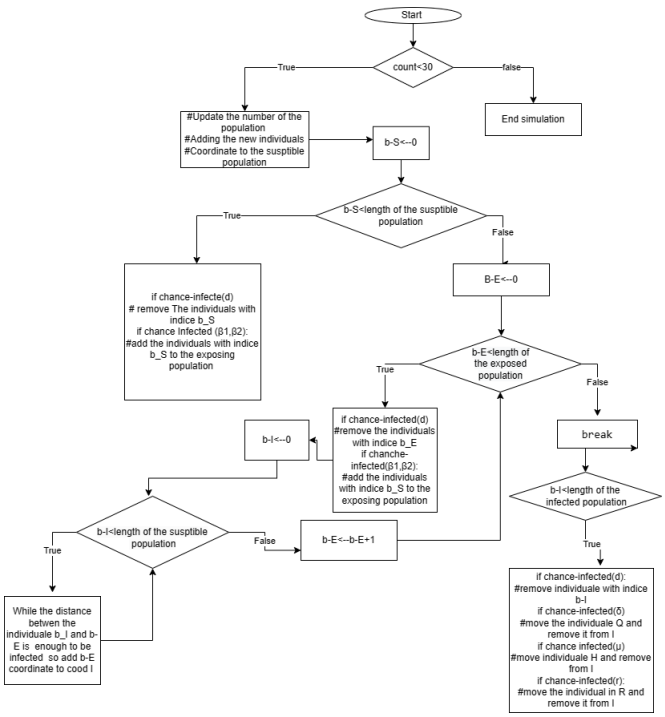

FIGURE 3. The clustering process for two compartments.

(b) The same process applies to the remaining individuals.

(4) Step 4

(a) In our case, we used the Plotly library only to manage multiple plots but used matplotlib to draw the curves (using scatter function).

3. RESULTS AND DISCUSSION

In this section, we illustrate the numerical simulations and explore the two approaches that we adopted (mathematical and computational) to make predictions and obtain graphical representations. Here, using the parameter values in Tables 2 and 3, which were mostly borrowed

from the literature [13], we perform some simulations to numerically illustrate our theoretical results. Then, we evaluate the impact of two parameters (transmission rate; infection rate of infected and exposed individuals) on the transmission dynamics of the disease.

3.1. Simulation with different R_0.

We will perform numerical simulations for both cases: disease-free ($R_0 < 1$) and endemic equilibria ($R_0 > 1$).

We vary the basic reproduction rate R_0 of our mathematical model (2.1), whose expression is as follows:
$R_0 = \frac{\Lambda(\beta_1\alpha+\beta_2(\delta+\mu+\eta+d))}{(d+a_s)(\delta+\mu+\eta+d)(\alpha+d)}$. We consider the following two cases:

Case 1: $R_0 = 0.9504 < 1$

Table 2 below shows the various parameters' values for a $R_0 = 0.9504 < 1$.

Parameters	Values
Λ	80
β_1	0.001
β_2	0.002
α	0.26
δ	0.33
d	0.001
μ	0.33
η	0.13
ε	0.12
r	0.014
a_s	0.75
a_r	0.5

TABLE 2. Values of parameters for $R_0 < 1$

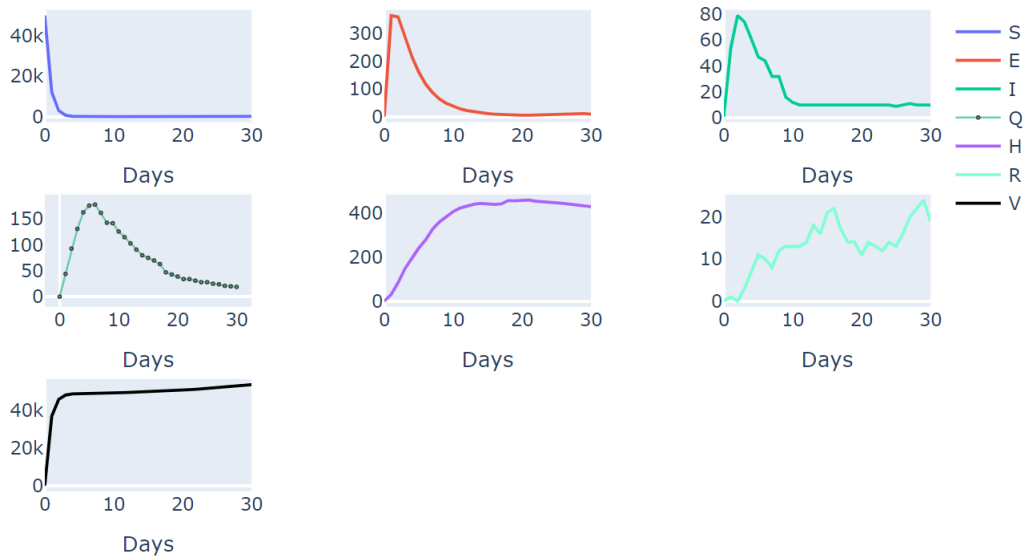

FIGURE 4. Curves of computational model for $R_0 < 1$

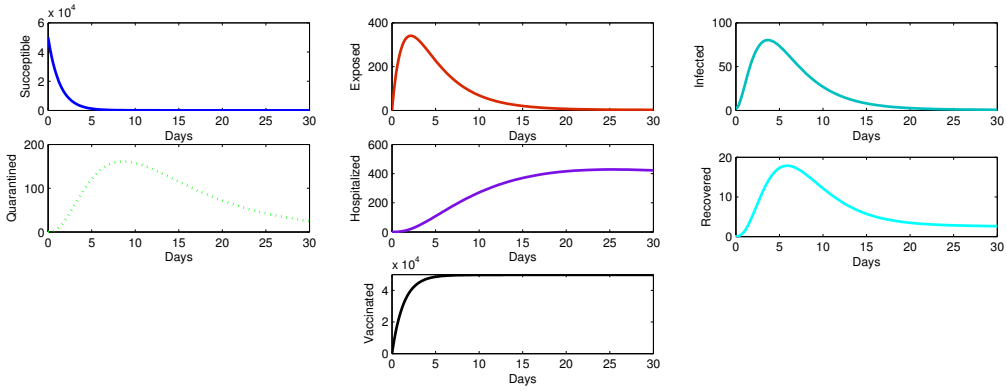

FIGURE 5. Curves of mathematical model for $R_0 < 1$

The curves for the seven compartments of daily COVID-19 cases are reported for both models (see Figures 4 and 5). In this case, the fact that $R_0 < 1$ indicates that the risk of infection is relatively low over the 30-day period, due to the containment of individuals that greatly limits inter-human and inter-environmental contact and effectively weakens all routes of virus transmission, leading to fewer infected individuals, which in turn weakens the spread of the virus. Thus, the peak number of people affected is relatively low. We can therefore say that the epidemic is under control on a global scale.

Case 2: $R_0 = 1.118 > 1$

With the values of the parameters indicated in the table below (Table 3), we obtain the following: $R_0 = 1.118$.

Parameters	Values
Λ	100
β_1	0.001
β_2	0.002
α	0.26
δ	0.33
d	0.001
μ	0.33
η	0.13
ε	0.12
r	0.014
a_s	0.75
a_r	0.5

TABLE 3. Values of Parameters for $R_0 = 1.118 > 1$

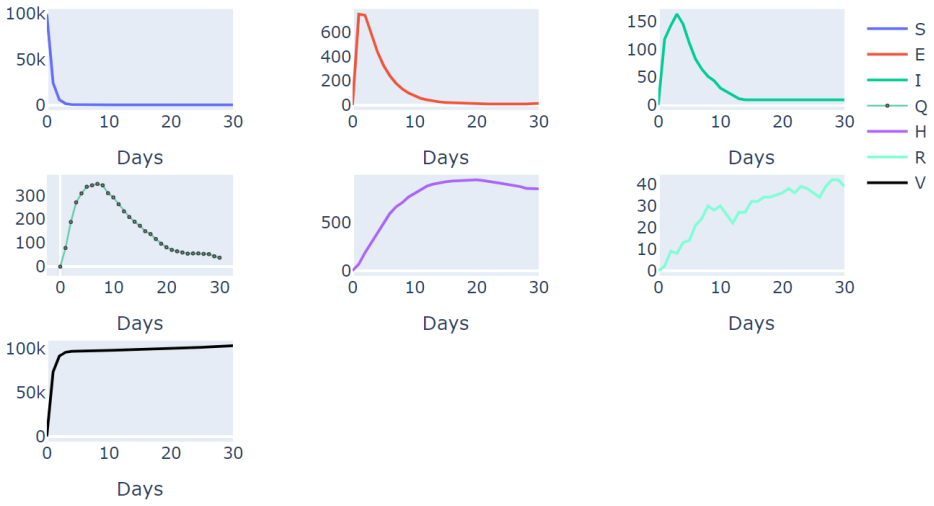

FIGURE 6. Curves of computational model for $R_0 > 1$

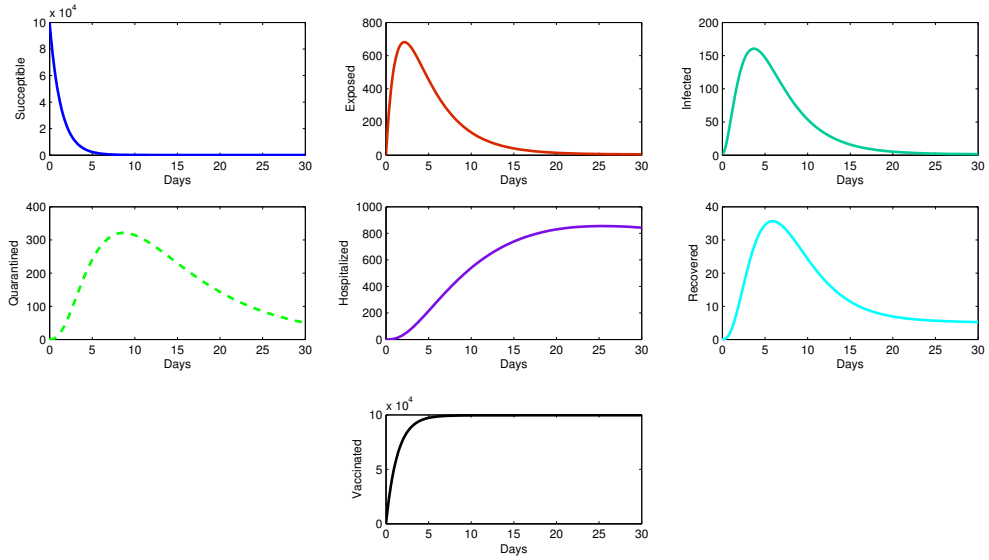

FIGURE 7. Curves of mathematical model for $R_0 > 1$

Figures 6 and 7 illustrate the mathematical and computational models that represent the curves of each observed daily compartment. As a result of increased human activity and a rise in the number of Λ individuals (relative to case 1), the transmission of the virus has increased in this scenario, meaning there will be more incidences of infection. As R_0 increases, the virus spreads faster and with high significance.

Model validation:

Let us first observe the results (the graphs) for the mathematical model SEIQHRV and the computational model created using Python by taking two values of R_0, one lower and the other higher than 1. For the two cases of simulations carried out, the values of the common parameters are identical for the two models (mathematical and computational). We can see that the curves of the individuals S, E, I, Q, H, and V are relatively similar in these two simulations for both values of R_0. However, the curve of recovered individuals R is a little more 'volatile' in our computational model. We will validate the COVID-19 model by using the mathematical model as a reference model. Among the seven curves found in the results of the two models, we will take the daily infected cases for the two cases (R_0¡1) and (R_0¿1). The graphs and the residuals

of the fit are presented in Figures 8 and 9, where it can be seen that the residuals are small and random. Thus, we can conclude that the fit is reasonably good [29].

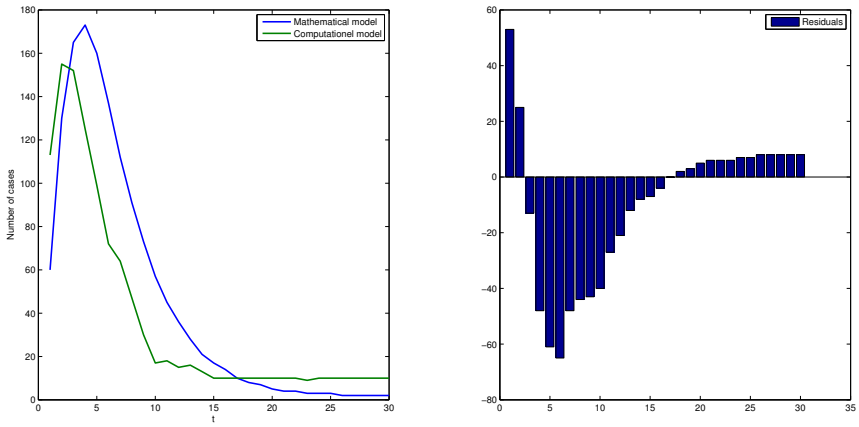

FIGURE 8. The residuals of the fit for $R_0 > 1$

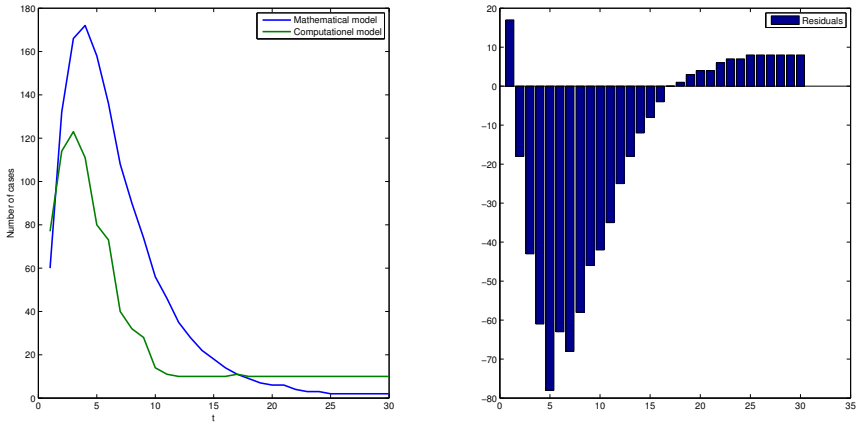

FIGURE 9. The residuals of the fit for $R_0 < 1$

3.2. Simulation with different infection rates.

We will study the impact of certain parameters (β_1, β_2) on the different states. To do this, we vary the infection rate β_1 between 0.001, 0.0030, and 0.005. The figure 10 shows the impact of the infection rate β_1 on all compartments. Over the first two days, the increase in the β_1 rate leads to an increase in exposed cases E, after which it rapidly decreases. Infected I, confined Q, and recovered R increase over the first four, six, and eight days, respectively. Thereafter,

they decrease rapidly. Hospitalised cases increase in line with the increase of the β_1 rate. In this figure 10, we can see that the β_1 rate has a weak impact on susceptible S and vaccinated V cases.

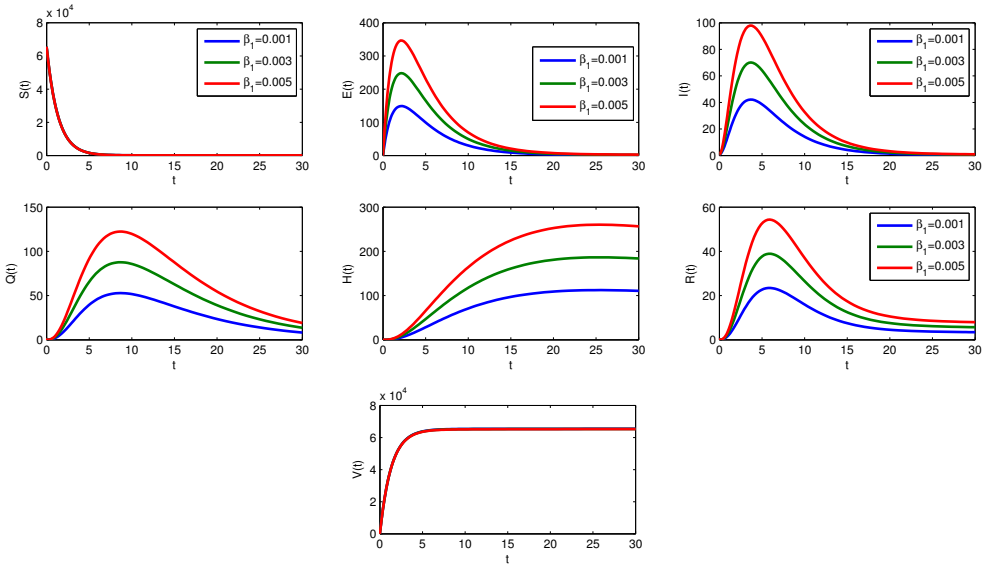

FIGURE 10. Solution curves corresponding to the set values parameters endemic equilibrium P with different values of β_1

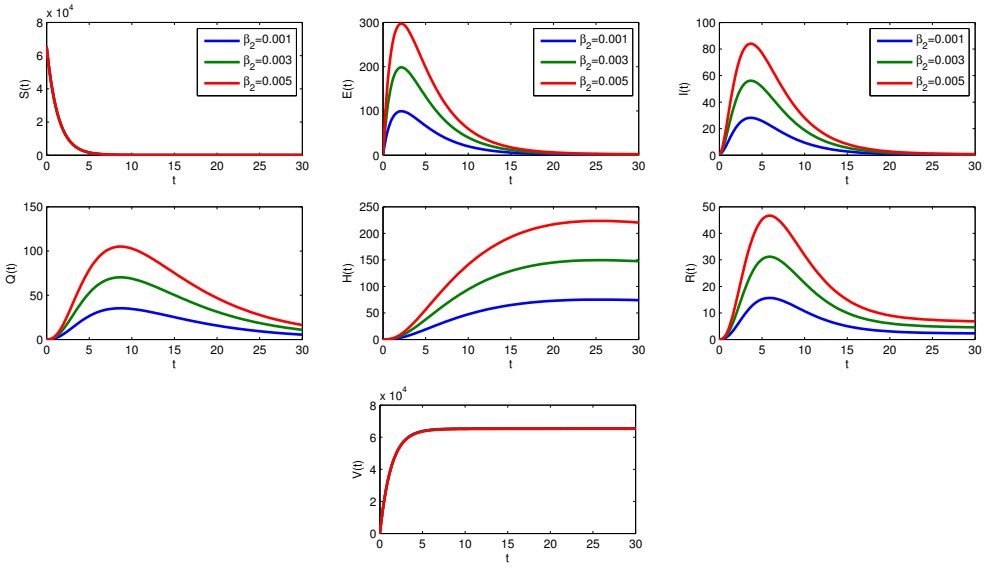

FIGURE 11. Solution curves corresponding to the set values parameters endemic equilibrium P with different values of β_2

Figure 11 shows the impact of the infection rate β_2 on the seven compartments. From this we can see that β_2 has almost the same impact as β_1. Indeed, over the first three days, the β_2 rate rapidly increases in line with the number of exposed cases E, before quickly falling. Infected I, quarantined Q, and recovered R increase over the first four, seven, and nine days, respectively, and then decrease rapidly. The curves of hospitalised cases, meanwhile, are almost linear for a long period, before converging to the steady state. The difference lies in the speed of convergence at which the threshold is reached; that is, the higher the infection rate of the exposed cases β_2, the faster the threshold (the steady state) is reached. Thus, we can conclude that the β_2 rate has a negligible impact on the susceptible S and vaccinated V cases. This confirms the theoretical solutions because it shows that they will converge to the equilibrium point (see equation (2.4)).

We conclude that the higher the infectivity (β_1 and β_2), the higher the maximum number (the peak) of infected cases. After that peak is reached, though, the number of infected cases falls rapidly.

3.3. Comparing the two measures: β_1 and β_2.

The sensitivity analysis demonstrates the effect of each parameter on the spread of the disease. It enables us to understand which variables significantly influence the threshold of R_0. In particular, sensitivity indices measure the proportional variation of a variable when a parameter changes. If this variable is differentiable with respect to the parameter a, the sensitivity index is defined as follows: [30]:

$$S_a^{R_0} = \frac{\partial R_0}{\partial a}\frac{a}{R_0}$$

where a is the contribution with respect to R_0. For the parameters β_1 et β_2, we have:
$S_{\beta_1}^{R_0} = \frac{\beta_1\alpha}{\beta_1\alpha+\beta_2(\delta+\mu+\eta+d)}$ and $S_{\beta_1}^{R_0} = \frac{\beta_2(\delta+\mu+\eta+d)}{\beta_1\alpha+\beta_2(\delta+\mu+\eta+d)}$.
For example, using the values from Table 2, we obtain $S_{\beta_1}^{R_0} = 0.1412$ et $S_{\beta_2}^{R_0} = 0.8588$. In this case, the infection rate β_2 has a pronounced impact on the propagation of the virus.

In this study, we presented a computational model designed to improve our understanding of how a virus (COVID-19) behaves in a population, how specific parameters influence its spread, and how the evolution of the disease outbreak can be estimated. Furthermore, we presented a simulation of the model applied to a set of random individuals, before evaluating and validating

our model by comparing these results with those of the proposed mathematical model (2.1). In addition, we analysed the dynamic evolution of the disease over time by varying some parameters. Finally, we compared the curves of the results of each case with the curves obtained using the SEIQHRV mathematical model. This research aimed to validate predictions regarding the effect of specific parameters on the behaviour of COVID-19 and in so doing improve our understanding of the virus.

In our analysis, we observed that the model we created is easy to manipulate when tested and that the curves it produced are relatively similar for the two models in the different cases studied. Hence, the reliability of the model was confirmed, meaning that these results can be used to aid in the decision-making process of specialists in the field of epidemiology.

Indeed, the results of the compartmental models have already been exploited in some studies by medical doctors [31] and epidemiologists. It is reasonable to suppose, then, that the computational model can be easily manipulated in various studies that are focused only on the results (numerical simulation) without any need for the complicated mathematical calculations of the mathematical models, especially in the fields that rely on this type of results (the estimation of the evolution of individuals in each compartment in the course of time) to be exploited. The use of this kind of method will facilitate the work of specialists and allow health officials to more effectively determine precautionary and suitable measures of action to combat the epidemic. This approach can be applied in future research to model several infectious diseases that are currently modeled using compartmental mathematical models.

To the best of our knowledge, this report is the first to use a Python model that can be easily applied to study the dynamic evolution of COVID-19 in a way similar to that achieved by compartmental model results in epidemiology. Although the proposed computational model is not yet suitable for practical use, we have published instructions for implementing the model as part of the open initiative in order to encourage widespread use and improvement within the research community.

4. CONCLUSION

In order to help researchers build new, easy-to-use, and efficient prediction techniques for common diseases, as well as to extend prediction methodologies and overcome the technical

limitations of mathematical models, we created a computational model (programmed in Python) that can be easily used to predict the growth of the COVID-19 population and to estimate the evolution of the epidemic.

It should be noted, however, that this epidemiological study remains highly theoretical in a deeply realistic field. In other words, even if the results and observations obtained by the Python model appear to be relatively close to reality (mathematical model), it should be borne in mind that these models do not take into account certain key factors, such as the different types of vaccination, the quarantine of individuals immediately after they are infected, or even the movement of individuals in the population. Nevertheless, such a study does help us to understand how a virus behaves in a population, measure the influence of certain factors on the virus's propagation, and to estimate the evolution of the epidemic.

Thus, these kinds of models are crucial because performance, speed, and simplicity are essential metrics in improving forecasting methods without the need for sophisticated equipment and resources. Mathematical modeling approaches are rapidly becoming better at facilitating epidemiological studies in the current pandemic, which may represent a step toward a developed forecasting system, which could form rapid predictions, be beneficial in eliminating the risk of such pandemics ever starting in the first place, and offer tremendous opportunities to harmonize sustainable development goals.

CONFLICT OF INTERESTS

The author(s) declare that there is no conflict of interests.

REFERENCES

[1] https://www.worldometers.info/coronavirus/

[2] L. Durán-Polanco, M. Siller, Crowd management COVID-19, Ann. Rev. Control. 52 (2021), 465-478. https://doi.org/10.1016/j.arcontrol.2021.04.006.

[3] S. Annas, Muh. Isbar Pratama, Muh. Rifandi, W. Sanusi, S. Side, Stability analysis and numerical simulation of SEIR model for pandemic COVID-19 spread in Indonesia, Chaos Solitons Fractals. 139 (2020), 110072. https://doi.org/10.1016/j.chaos.2020.110072.

[4] A.A. Mohsen, H.F. AL-Husseiny, K. Hattaf, B. Boulfoul, A mathematical model for the dynamics of COVID-19 pandemic involving the infective immigrants, Iraqi J. Sci. 62 (2021), 295-307. https://doi.org/10.24996/ijs.2021.62.1.28.

[5] J. Arino, S. Portet, A simple model for COVID-19, Infect. Dis. Model. 5 (2020), 309-315. https://doi.org/10.1016/j.idm.2020.04.002.

[6] C. Yang, J. Wang, Modeling the transmission of COVID-19 in the US - A case study, Infect. Dis. Model. 6 (2021), 195-211. https://doi.org/10.1016/j.idm.2020.12.006.

[7] R.W. Mbogo, T.O. Orwa, SARS-COV-2 outbreak and control in Kenya - Mathematical model analysis, Infect. Dis. Model. 6 (2021), 370-380. https://doi.org/10.1016/j.idm.2021.01.009.

[8] S.S. Musa, S. Qureshi, S. Zhao, et al. Mathematical modeling of COVID-19 epidemic with effect of awareness programs, Infect. Dis. Model. 6 (2021), 448-460. https://doi.org/10.1016/j.idm.2021.01.012.

[9] M.Y. Li, J.S. Muldowney, Global stability for the SEIR model in epidemiology, Math. Biosci. 125 (1995), 155-164. https://doi.org/10.1016/0025-5564(95)92756-5.

[10] Y. Zhang, B. Jiang, J. Yuan, et al. The impact of social distancing and epicenter lockdown on the COVID-19 epidemic in mainland China: A data-driven SEIQR model study, preprint, (2020). https://doi.org/10.1101/2020.03.04.20031187.

[11] C. Xu, Y. Yu, Y. Chen, et al. Forecast analysis of the epidemics trend of COVID-19 in the USA by a generalized fractional-order SEIR model, Nonlinear Dyn. 101 (2020), 1621-1634. https://doi.org/10.1007/s11071-020-05946-3.

[12] M. Elhia, K. Chokri, M. Alkama, Optimal control and free optimal time problem for a COVID-19 model with saturated vaccination function, Commun. Math. Biol. Neurosci. 2021 (2021), 35. https://doi.org/10.28919/cmbn/5632.

[13] S.A. Ould Beinane, M.R. Lemnaouar, R. Zine, Y. Louartassi, Stability analysis of COVID-19 epidemic model of type SEIQHR with fractional order, Math. Probl. Eng. 2022 (2022), 5163609. https://doi.org/10.1155/2022/5163609.

[14] E. Fayyoumi, S. Idwan, H. AboShindi, Machine learning and statistical modelling for prediction of novel COVID-19 patients case study: Jordan, Int. J. Adv. Computer Sci. Appl. 11 (2020), 122-126.

[15] I. Rahimi, F. Chen, A.H. Gandomi, A review on COVID-19 forecasting models, Neural Comput. Appl. (2021). https://doi.org/10.1007/s00521-020-05626-8.

[16] J.C. Clement, V. Ponnusamy, K.C. Sriharipriya, et al. A Survey on Mathematical, Machine learning and deep learning models for COVID-19 transmission and diagnosis, IEEE Rev. Biomed. Eng. 15 (2022), 325-340. https://doi.org/10.1109/rbme.2021.3069213.

[17] T. Chakraborty, I. Ghosh, Real-time forecasts and risk assessment of novel coronavirus (COVID-19) cases: A data-driven analysis, Chaos Solitons Fractals. 135 (2020), 109850. https://doi.org/10.1016/j.chaos.2020.109850.

[18] V.K.R. Chimmula, L. Zhang, Time series forecasting of COVID-19 transmission in Canada using LSTM networks, Chaos Solitons Fractals. 135 (2020), 109864. https://doi.org/10.1016/j.chaos.2020.109864.

[19] S.J. Fong, G. Li, N. Dey, et al. Finding an accurate early forecasting model from small dataset: a case of 2019-nCoV novel coronavirus outbreak, Int. J. Interact. Multimedia Artif. Intell. 6 (2020), 132-140. https://doi.org/10.9781/ijimai.2020.02.002.

[20] M.A.A. Al-qaness, A.A. Ewees, H. Fan, et al. Optimization method for forecasting confirmed cases of COVID-19 in China, J. Clinic. Med. 9 (2020), 674. https://doi.org/10.3390/jcm9030674.

[21] D. Parbat, M. Chakraborty, A python based support vector regression model for prediction of COVID19 cases in India, Chaos Solitons Fractals. 138 (2020), 109942. https://doi.org/10.1016/j.chaos.2020.109942.

[22] I. Rahimi, F. Chen, A.H. Gandomi, A review on COVID-19 forecasting models, Neural Comput. Appl. (2021). https://doi.org/10.1007/s00521-020-05626-8.

[23] L. Xu, R. Magar, A. Barati Farimani, Forecasting COVID-19 new cases using deep learning methods, Computers Biol. Med. 144 (2022), 105342. https://doi.org/10.1016/j.compbiomed.2022.105342.

[24] W. Jin, S. Dong, C. Yu, et al. A data-driven hybrid ensemble AI model for COVID-19 infection forecast using multiple neural networks and reinforced learning, Computers Biol. Med. 146 (2022), 105560. https://doi.org/10.1016/j.compbiomed.2022.105560.

[25] https://plotly.com/python/getting-started.

[26] H.A. Antosiewicz, Ordinary differential equations (G. Birkhoff and G. C. Rota), SIAM Rev. 5 (1963), 160-161. https://doi.org/10.1137/1005043.

[27] Y. Louartassi, E.H. El Mazoudi, N. Elalami, et al. A new generalization of lemma Gronwall-Bellman, Appl. Math. Sci. 6 (2012), 621-628.

[28] F. Pedregosa, G. Varoquaux, A. Gramfort, et al. Scikit-learn: Machine learning in Python, J. Mach. Learn. Res. 12 (2011), 2825-2830. https://cir.nii.ac.jp/crid/1370005891170856713.

[29] M. Martcheva, An introduction to mathematical epidemiology, Springer, New York, 2015. https://doi.org/10.1007/978-1-4899-7612-3.

[30] S. Osman, O.D. Makinde, D.M. Theuri, Stability analysis and modelling of listeriosis dynamics in human and animal populations, Glob. J. Pure Appl. Math. 14 (2018), 115-137.

[31] M.A. Abdul Rasheed, M.M.J. Farooque, H.S. Acharya, et al. Mathematical modelling of the relationship between two different temperament classifications: during the Covid-19 pandemic, Emerg. Sci. J. 5 (2021), 67-76. https://doi.org/10.28991/esj-2021-01258.